Int. J. Heat Mass Transfer. Vol. 32, No. 11, pp. 2037–2046, 1989
Printed in Great Britain

0017–9310/89 $3.00 + 0.00
Pergamon Press plc

Application of a gradient diffusion and dissipation time scale ratio model for prediction of mean and fluctuating temperature fields in liquid sodium downstream of a multi-bore jet block

K. BREMHORST,† L. KREBS,‡ U. MÜLLER‡ and J. B. H. LISTIJONO†

†Department of Mechanical Engineering, University of Queensland, St. Lucia, Queensland 4067, Australia

‡Kernforschungszentrum Karlsruhe, Institut für Reaktorbauelemente, Postfach 3640, 7500 Karlsruhe, Federal Republic of Germany

(*Received* 4 *January* 1989 *and in final form* 2 *March* 1989)

Abstract—A previously developed diffusivity based model, for the prediction of mean and fluctuating temperatures in water flow downstream of a multi-bore jet block in which one jet is heated, is applied to a flow of sodium in apparatus of similar geometry. Some measurements not readily possible in sodium or water flows for this geometry are made using air in order to verify assumptions used in the model. The earlier derived mathematical model is modified to remove assumptions relating to turbulence Reynolds number and turbulence Peclet number in the relationship between velocity and temperature microscales. Spalding's model, relating fluctuating velocity and temperature dissipation rates, is tested. A significant effect on this relationship due to the low Prandtl number of liquid sodium is identified. Measurements performed behind a multi-bore jet block with air as the working fluid have verified the non-isotropic nature of the large-scale flow. Results clearly show that measurements performed in water can be transferred to liquid sodium provided that molecular diffusion is included in the mean temperature equation, allowance is made for the Prandtl number effect on the dissipation time scale ratio and the coefficient of gradient diffusion of mean square temperature fluctuations is assumed equal to the eddy diffusivity of heat.

1. INTRODUCTION

COOLANT flow monitoring in fuel rod sub-assemblies of sodium cooled nuclear reactors requires reliable instrumentation for velocity measurements. Since the latter is not available at this stage, it is necessary to deduce coolant flow by means of mean and fluctuating temperature measurements obtained with the aid of thermocouples. Mathematical models must then be used to give some insight into the velocity field from temperature data. Laboratory studies of sodium cooled reactor geometries are generally carried out with water because dynamic similarity is easily achieved using the same or similar geometry, but few studies exist where the same geometries have been tested using both media. Although fuel rod assemblies consist of solid rods, separated by complicated voids through which the cooling medium flows, in the present study this situation is simulated by means of a multi-bore jet block set in a containment pipe (Fig. 1). The geometry of the flow cross-section is inverse to that in the rod bundle, but downstream flow can be expected to be similar in both cases as well as being similar to that found behind turbulence generating grids. It is to be expected, therefore, that turbulence levels, although high at the tube bundle or jet block exit, will decay rapidly, due to the absence of production of turbulence. Consequently, quite low levels of turbulence will exist over a large part of the flow domain of immediate interest.

Comte-Bellot and Corrsin [1] have shown that for the grid case, power laws are appropriate for the description of turbulence decay. Unfortunately, the exponents of such power laws are geometry dependent. It is necessary, therefore, to establish appropriate decay constants for each geometry under investigation. Decay of temperature fluctuations can also be represented by a power law. Warhaft and Lumley [2] have shown that the decay exponent for temperature fluctuations depends not only on geometry, but also on the method of heating, with a consequent large range of time scale ratios relating turbulence energy dissipation and temperature fluctuation dissipation, thus throwing doubt on a universal value for this ratio. The effect of a large change in Prandtl number on this time scale ratio does not appear to have been investigated.

Geometries similar to the present one have been studied by Brodkey [3] and Gad-el-Hak and Morton [4], but in both cases blockage ratios are significantly different as also are the geometric details. Furthermore, mathematical models for those flows have not been produced and tested. In the present work an eddy diffusivity approach has been used to solve the mean temperature equation. A gradient diffusion model and dissipation time scale ratio have been used to provide an equation which can be solved for mean square temperature fluctuation. The case of negligible molecular conductivity has already been presented in ref. [5]. The purpose of this paper is to extend that work to include cases of high molecular conductivity such as found in liquid metal flows and to check for

NOMENCLATURE

a eddy diffusivity of δ^2 [$m^2 s^{-1}$]
A_1, A_2, A_3, A_4 constants of proportionality
d diameter of bores in jet block [mm]
D diameter of containment pipe [mm]
E_1, E_2 potential [V]
L axial length of jet block [mm]
L_f Eulerian integral length scale, $(u')^{-1}\int_0^\infty \overline{u(x)u(x+\xi)}\,d\xi$ [mm]
m exponent in power law for $\overline{\delta^2}$
M pitch of holes in jet block [mm]
n exponent in power law for eddy diffusivity
n_1 exponent in power law for u^2
n_2 exponent in power law for L_f
Pr Prandtl number
q^2 twice the instantaneous turbulent energy [$m^2 s^{-2}$]
r radial coordinate [mm]
$r_{1/2}$ half value radius—radius at which the variable is half that at the centreline [mm]
R dissipation time scale ratio, equation (10)
Re_M Reynolds number based on bulk velocity in containment pipe and mesh size
S volume flow of heated jet [$mm^3 s^{-1}$]
$\bar{T}$ mean temperature at a point [K]
$\bar{T}_E$ bulk mean temperature of the heated jet at the exit of the jet block [K]
$\bar{T}_k$ mean temperature of unheated fluid in the test section [K]
u velocity fluctuation in the x-direction [$m s^{-1}$]
v velocity fluctuation in the r-direction [$m s^{-1}$]
$\bar{U}$ mean streamwise velocity at the flow cross-section [$m s^{-1}$]
$\bar{U}_i$ mean velocity in direction i [$m s^{-1}$]
$\bar{U}_0$ mean velocity in the containment pipe [$m s^{-1}$]
x streamwise coordinate, same as x_1 in the tensor formulation
x_i coordinate in direction i [mm]
x_{01}, x_{02}, x_{03} effective origins of $\overline{u^2}$, L_f and $\overline{\delta_m^2}$ [mm].

Subscripts
H_2O water
i coordinate directions 1, 2 and 3 corresponding to x, r and azimuthal direction
m maximum value at a given axial location
Na sodium.

Superscripts
$\bar{}$ time averaging
$'$ r.m.s. value.

Greek symbols
α molecular diffusivity of heat [$mm^2 s^{-1}$]
α_F eddy diffusivity of heat [$mm^2 s^{-1}$]
$\alpha_F(x)$ eddy diffusivity of heat assumed as a function of x [$mm^2 s^{-1}$]
δ stream temperature fluctuation [K]
δ'_{mo} maximum r.m.s. temperature fluctuation—measured near the exit of the block [K]
ε dissipation of velocity fluctuations [$mm^2 s^{-3}$]
ε_δ destruction or dissipation of temperature fluctuations [$K^2 s^{-1}$]
λ_f velocity microscale [mm]
Λ characteristic turbulence length scale
ν kinematic viscosity [$mm^2 s^{-1}$]
π 3.14...
v characteristic turbulent velocity.

flow anisotropy by means of measurements in air. This latter step was taken as hot-wire anemometers in air gave far better signal-to-noise ratios than hot-film anemometers in water at the very low level of velocity fluctuations found in a large part of the flow. Assumptions used previously involving turbulence Reynolds number and turbulence Peclet number have been removed by use of a power law decay model for turbulence energy and the dissipation time scale ratio.

2. MATHEMATICAL MODEL

The aim is to test a mathematical model using gradient diffusion approximations and a dissipation time scale ratio for calculation of mean flow temperature and temperature fluctuation distributions in the flow field downstream of a fuel rod subassembly. In particular, it is desired to check for any Prandtl number effects so that laboratory studies performed with more convenient working fluids than liquid sodium, can be transferred to the latter with confidence. Basic flow variables and the coordinate system are shown in Fig. 1 which also depicts the simplified geometry used to represent the flow situation of interest. Since only fluid in the central bore is heated, it will be assumed throughout that the resultant thermal wake or jet is sufficiently small in radial extent so that it is not influenced by any boundary layer forming on the containment pipe wall.

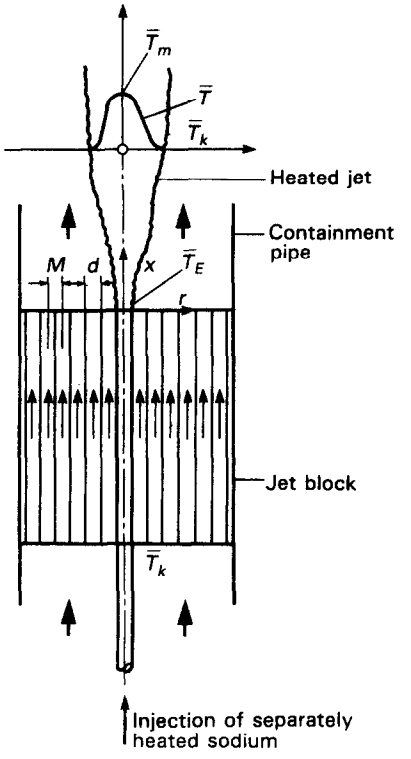

FIG. 1. Multi-bore jet block and coordinate system.

2.1. *Mean temperature field*

For steady, incompressible flow with negligible heating by dissipation and no internal heat sources, the energy equation reduces to the general form

$$\bar{U}_i \frac{\partial \bar{T}}{\partial x_i} = \frac{\partial}{\mathrm{d}x_i}\left[\alpha \frac{\partial \bar{T}}{\partial x_i} - \overline{u_i \delta}\right] \tag{1}$$

where the usual Reynolds decomposition has been used and the Einstein summation convention applies to repeated indices. Introducing the Boussinesq or gradient diffusion approximation, equation (2), into equation (1) leads to equation (3). The eddy diffusivity of heat, α_E, in these two equations is assumed to be a scalar

$$\overline{u_i \delta} = -\alpha_E \frac{\partial \bar{T}}{\partial x_i} \tag{2}$$

$$\bar{U}_i \frac{\partial \bar{T}}{\partial x_i} = \frac{\partial}{\partial x_i}[\alpha + \alpha_E] \frac{\partial \bar{T}}{\partial x_i}. \tag{3}$$

Use of a turbulent Prandtl number to relate eddy diffusivity of heat to eddy diffusivity of momentum, in order to achieve closure of equation (3), is inappropriate since a radial mean velocity gradient does not exist. If it is assumed that temperature is a passive scalar, than a model for the eddy diffusivity of heat can be obtained in terms of the velocity field by using the Lagrangian description of diffusion as a starting point [5]. This leads to the result

$$\alpha_E = \upsilon \Lambda \tag{4}$$

where υ is a characteristic turbulent velocity and Λ is a characteristic turbulence length scale.

Assuming that these are given by the streamwise velocity fluctuation and its integral length scale and if both display a power law dependence on distance downstream, equations (5a) and (5b), then α_E can be written as equation (5c) where $A_3 = A_2 \sqrt{A_1}$, $x_{01} = x_{02} = 0$ and $n - 1 = -n_1/2 + n_2$. A_3 and n can be obtained from experimental data

$$\frac{\overline{u^2}}{\bar{U}^2} = A_1 \left[\frac{x}{d} - \frac{x_{01}}{d}\right]^{-n_1} \tag{5a}$$

$$\frac{L_f}{d} = A_2 \left[\frac{x}{d} - \frac{x_{02}}{d}\right]^{n_2} \tag{5b}$$

$$\frac{\alpha_E}{\bar{U} d} = A_3 \left[\frac{x}{d}\right]^{n-1}. \tag{5c}$$

Except within the first 10–15 hole diameters of the exit, the velocity field is homogeneous in the radial and azimuthal directions. Consequently, the eddy diffusivity is a function only of the streamwise direction which will be emphasized by use of $\alpha_E(x)$ rather than α_E. If changes in $\bar{T}$ are more rapid in the radial direction than in the other two and if α and $\alpha_E(x)$ are independent of temperature, then equation (3) reduces to

$$\bar{U} \frac{\partial \bar{T}}{\partial x} = [\alpha + \alpha_E(x)]\left[\frac{1}{r}\frac{\partial \bar{T}}{\partial r} + \frac{\partial^2 \bar{T}}{\partial r^2}\right]. \tag{6}$$

For points at $x/d > 5$ and $r^2 \ll x^2$, the solution of equation (6) is given by

$$\frac{\bar{T} - \bar{T}_k}{\bar{T}_E - \bar{T}_k} \simeq \frac{S}{4\pi\left[\alpha + \frac{1}{n}\alpha_E(x)\right]x} \times \exp\left[-\frac{\bar{U}}{4\left[\alpha + \frac{1}{n}\alpha_E(x)\right]x} r^2\right] \tag{7}$$

where for large radii $\bar{T} = \bar{T}_k$, S is the volume flow of the heated jet and $\bar{T}_E$ the mean temperature of the heated jet at the jet block exit plane.

2.2. *Fluctuating temperature field*

The steady-state balance for temperature fluctuations is [6]

$$\bar{U}_i \frac{\partial \overline{\delta^2}}{\partial x_i} = -\overline{2u_i \delta} \frac{\partial \bar{T}}{\partial x_i} - \frac{\partial \overline{u_i \delta^2}}{\partial x_i} + \frac{\partial}{\partial x_i}\left(\alpha \frac{\partial \overline{\delta^2}}{\partial x_i}\right) - 2\alpha \overline{\frac{\partial \delta}{\partial x_i}\frac{\partial \delta}{\partial x_i}} \tag{8}$$

where $\overline{u_i \delta}$ and $\overline{u_i \delta^2}$ are modelled by the gradient diffusion approximations of equations (2) and (9), respectively

$$\overline{u_i\delta^2} = -a\frac{\partial\overline{\delta^2}}{\partial x_i}. \quad (9)$$

It will be assumed that $a = \alpha_E$ as used in refs. [7, 8].

For closure of the available set of equations, it is also necessary to introduce an assumption relating to the dissipation term, the last term of equation (8). Spalding [9] achieved this by introduction of the dissipation time scale ratio, R, relating $\overline{\delta^2}$ dissipation to turbulent kinetic energy dissipation

$$R = \frac{\varepsilon\overline{\delta^2}}{\overline{q^2}\varepsilon_\delta} \quad (10)$$

where $2\varepsilon_\delta$ equals the last term of equation (8) and R is assumed to be a constant with a value of 0.833 for grid flows and 0.5 for shear flows [8]. Equation (8), therefore, simplifies in its modelled form to equation (11) which can be solved for R using experimentally determined profiles of $\overline{\delta^2}$

$$\bar{U}_i\frac{\partial\overline{\delta^2}}{\partial x_i} = 2\alpha_E\left(\frac{\partial\bar{T}}{\partial x_i}\right)^2 + \frac{\partial}{\partial x_i}\left[(\alpha+\alpha_E)\frac{\partial\overline{\delta^2}}{\partial x_i}\right] - \frac{2\varepsilon\overline{\delta^2}}{R\overline{q^2}}. \quad (11)$$

Further simplification is possible if it is assumed that:

(a) $$\bar{U}\frac{\partial\overline{\delta^2}}{\partial x} \gg \frac{\partial\alpha_E}{\partial x_i}\frac{\partial\overline{\delta^2}}{\partial x_i};$$

(b) $$\frac{\partial^2\overline{\delta^2}}{\partial x^2} \ll \frac{1}{r}\frac{\partial}{\partial r}\left(r\frac{\partial\overline{\delta^2}}{\partial r}\right);$$

(c) the velocity field is isotropic so that

$$\overline{q^2} = 3\overline{u^2}$$

and

$$\varepsilon = -\frac{3}{2}\bar{U}\frac{d\overline{u^2}}{dx}$$

where use of the decay law for $\overline{u^2}$ of equation (5a) leads to

$$\frac{\varepsilon}{\overline{q^2}} = \frac{n_1\bar{U}}{2(x-x_{01})}.$$

Equation (12) then gives the final working result in cylindrical coordinates where the x dependence of α_E, as in equation (6), has been included

$$\bar{U}\frac{\partial\overline{\delta^2}}{\partial x} = \alpha_E(x)\left[2\left(\frac{\partial\bar{T}}{\partial x}\right)^2 + 2\left(\frac{\partial\bar{T}}{\partial r}\right)^2\right] + [\alpha+\alpha_E(x)]\left[\frac{\partial^2\overline{\delta^2}}{\partial r^2} + \frac{1}{r}\frac{\partial\overline{\delta^2}}{\partial r}\right] - \frac{n_1\bar{U}\overline{\delta^2}}{R(x-x_{01})}. \quad (12)$$

The boundary conditions applying to equation (12) at the point $(x, D/2)$ are $\overline{\delta^2} = 0$ and $\partial\overline{\delta^2}/\partial r = 0$ where D is the diameter of the containment pipe or a radial distance sufficiently large to satisfy this condition.

In the present case, the velocity field approximates the results found in typical grid flows for which the exponent n_1 and the effective origin for equation (5a) are readily determined from velocity field measurements. Since heating of the flow is localized to the central bore, significant temperature gradients will result so that R cannot be obtained from the assumption of isotropy. It can, however, be found by solving equation (12) for various arbitrary values of R, and then selecting the one which gives the best fit to all δ^2 distributions in the flow field.

3. APPARATUS AND INSTRUMENTATION

Heated flow experiments were conducted with water and liquid sodium. Experimental details with water have already been described in ref. [5]. A similar test section geometry was used for experiments with sodium, but in order to avoid the need for axial movement of measurement sensors, the jet block was made moveable within the containment pipe, generally as shown in Fig. 2. In both cases, bores of 7.2 mm diameter placed on a triangular pitch of 8.2 mm with a length-to-diameter ratio of 16.7:1 were used, thus giving a blockage ratio (non-flow area relative to total area) of 30%. The containment pipe diameter was large enough to avoid interaction between the heated jet and any boundary layer forming on the wall of the containment pipe. Such effects would complicate the study unnecessarily. Heated fluid was injected into the centrally located bore ensuring that no mismatch of velocity with surrounding bores occurred. In order to minimize heat loss from heated sodium in the central bore, a double wall construction was used with the space between the walls being evacuated.

Velocity and temperature measurements in water were performed with hot-film and hot-wire anemometry [7]. For liquid sodium flows, mean temperature and temperature fluctuations were measured with a 0.25 mm o.d., sheathed thermocouple. The insulating material was boron nitride with a thermal con-

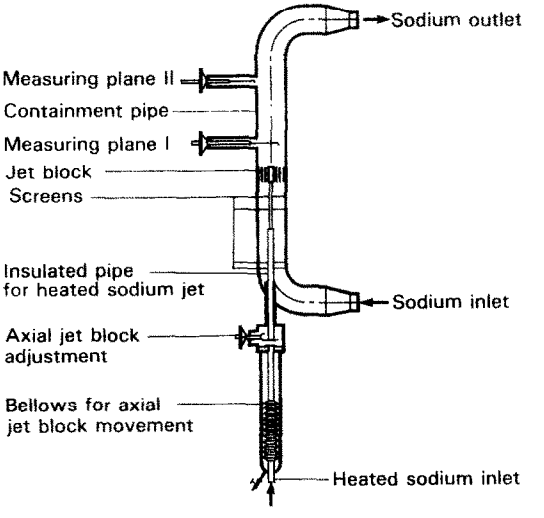

FIG. 2. Schematic of sodium test section.

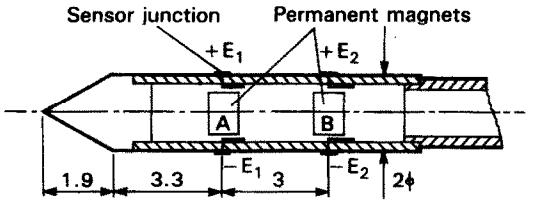

FIG. 3. Miniature electromagnetic flow meter probe, A and B are magnets—dimensions in mm.

ductivity equal to that of the stainless steel sheath. This ensures a small time constant with cut-off frequencies being in excess of 40 Hz which permits the energy containing part of the spectrum to be captured with minimal attenuation.

Velocity measurements, although extremely difficult to perform in liquid sodium, were made with a miniature permanent magnet flow meter probe, Fig. 3 and ref. [10]. Such a probe consists of two disc shaped magnets A and B with diametral magnetization. The discs are contained in a cladding tube which also carries positive and negative voltage electrodes. As conducting liquid sodium moves normal to the magnetic field, voltages are produced in the flow and are sensed by the electrodes. Although the magnetic field which permeates the surrounding fluid is not homogeneous, the voltage induced was found to be proportional to the flow velocity over a wide range of velocities. Typical sensitivities are of the order of 20 μV ms^{-1}. Unfortunately, dimensions of the probe are still somewhat large in relation to length scales of the flow. It must, therefore, be expected that mean velocity will be measured accurately, but turbulence measurements will be affected by lack of adequate spatial resolution.

Measurements with air were performed using a multi-bore jet block consisting of 8.7 mm diameter holes set on a diametral pitch of 9.9 mm all of which are set in a containment pipe of 132.9 mm diameter. The length-to-diameter ratio of the bores was again 16.7 : 1 and the blockage ratio was 30%, based on hole size and pitch.

Velocity measurements in air flow were performed with Disa 55M11 constant temperature anemometers with Wollaston type platinum–rhodium wire of 5 μm diameter and 1.2 mm long. Although turbulence levels were low, linearization was employed as it permitted easy correction for any temperature difference encountered between operating and calibrating conditions by the method described in ref. [11].

4. EXPERIMENTAL RESULTS

Since the jet block hole size or hole pitch, which corresponds to the mesh size of grids, determines flow characteristics, a mesh Reynolds number based on the bulk velocity in a hole, and the hole pitch is quoted. For sodium and water flows two Reynolds numbers were used in each case, Re_M = 17 070 and 34 140. In order to achieve the same Reynolds numbers in the two flows, velocities were adjusted in the ratio of the dynamic viscosities, that is, $\nu_{Na}/\nu_{H_2O} = 0.4$. Experiments with sodium were conducted at 300°C and those with water at 20°C, giving Prandtl numbers of 0.0058 and 7.01, respectively.

Decay of the mean temperature on the heated jet centreline is shown in Fig. 4 which also includes curves fitted to experimental data using equation (7) together with equation (5c). For water, the molecular conduction term was neglected ($\alpha = 0$) and n was taken to be 0.6 made up of $n_1 = 1.67$ and $n_2 = 0.44$ [7]. It is seen that the same curve applies for water at two different Reynolds numbers, thus verifying that molecular diffusivity effects are negligible, whereas for sodium, two curves are obtained. Thus, A_3 is essentially independent of Reynolds number but not of Prandtl number. The larger value of A_3 for water is consistent with the fact that lower molecular diffusion, leads to larger temperature length scales. This effect is neglected in the development of equation (5c).

Measured radial profiles of mean temperature are compared in Fig. 5 with calculated ones using the above experimental values of A_3. Excellent agreement is observed. The significant effect due to high molecular diffusivity of sodium is also clearly evidenced by wider tails of each distribution.

A measure of the decay of temperature fluctuations can be obtained from the decay of the peaks in the radial distribution (Fig. 6). For $x/d > 20$ a power law corresponding to equation (13) is observed. Equation (12) may now be used together with a known radial distribution of temperature fluctuation intensity to solve for the dissipation time scale ratio, R

$$\frac{\overline{\delta_m^2}}{\overline{\delta_{m0}^2}} = A_2\left(\frac{x}{d} - \frac{x_{03}}{d}\right)^{-m}. \qquad (13)$$

Figures 7 and 8 show the results of such computations where R obtained at $x/d = 28$ is applied to the remaining flow field with good agreement between predictions and measurements. A value of $x_{01} = 0$ was used in all cases. As for the mean temperature, Fig. 8 shows a single decay curve for water but with sodium a different one is obtained for each Reynolds number as α is no longer negligible relative to $\alpha_E(x)$ in equation (12). The temperature fluctuation decay exponent for equation (13) is also shown in Fig. 8.

A spectral analysis of temperature fluctuations in liquid sodium at the higher Reynolds number confirmed the adequacy of the thermocouple response. At 100 Hz, the power spectral density is already down to 10% of that at 10 Hz, the drop-off beginning at about 15–20 Hz.

As a check on turbulence in liquid sodium, the measurements of Fig. 9 were obtained with the electromagnetic probe. Somewhat lower turbulence levels than those measured in water are indicated together with a different slope. Since probe dimensions were of

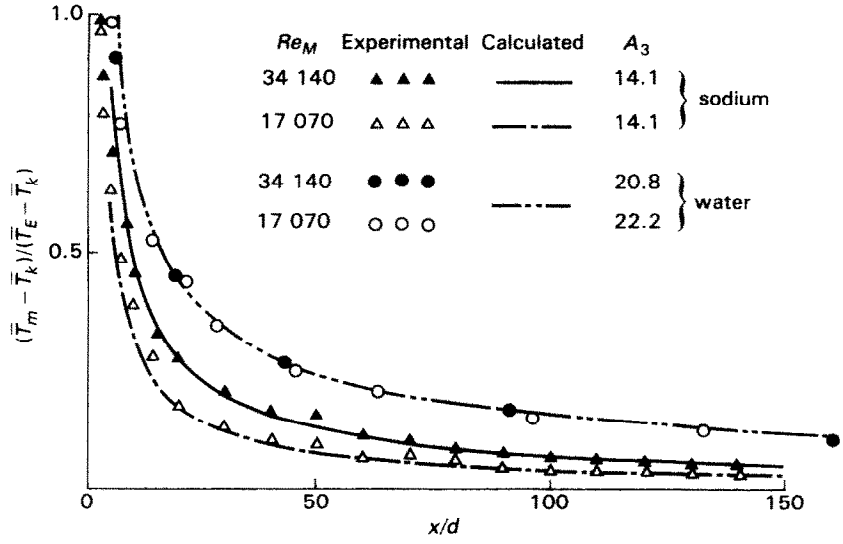

FIG. 4. Axial decay of centreline mean temperature.

similar size to the Taylor microscale and hence much larger than the Kolmogorov scale, significant probe size effects are to be expected. Measurements of the turbulence level behind a jet block using air (Fig. 9) confirmed measurements taken in water so that the decay constant $n_1 = 1.67$ can be taken as representative. Use of an effective origin gave a better straight line fit but was not considered worthwhile.

Model developments were based on velocity field isotropy. Figure 9 includes lateral turbulence levels measured in air. For most of the flow region of interest, the lateral turbulence level is seen to be 80% of the longitudinal one. Thus the flow is not fully isotropic but still follows the power law decay behaviour assumed throughout. Consequently, longitudinal turbulence velocity decay is larger than for isotropic turbulence due to transfer of energy to the other two turbulence components. For grid type flows n_1 is larger than the range of 1.18–1.39 reported by Comte-Bellot and Corrsin [1] but is consistent with the difference between streamwise and lateral turbulence levels thus again illustrating the dependence of n_1 on the geometry of the turbulence generator. Velocity microscales (Fig. 10) were obtained for water and air from turbulence spectra. These are seen to be similar, which is to be expected if the two flows are to be similar.

Measurements in air [12] showed negative skewness of u for $3 \leqslant x/d \leqslant 27$, slight positive skewness for $27 < x/d \leqslant 75$ and thereafter it again went slightly

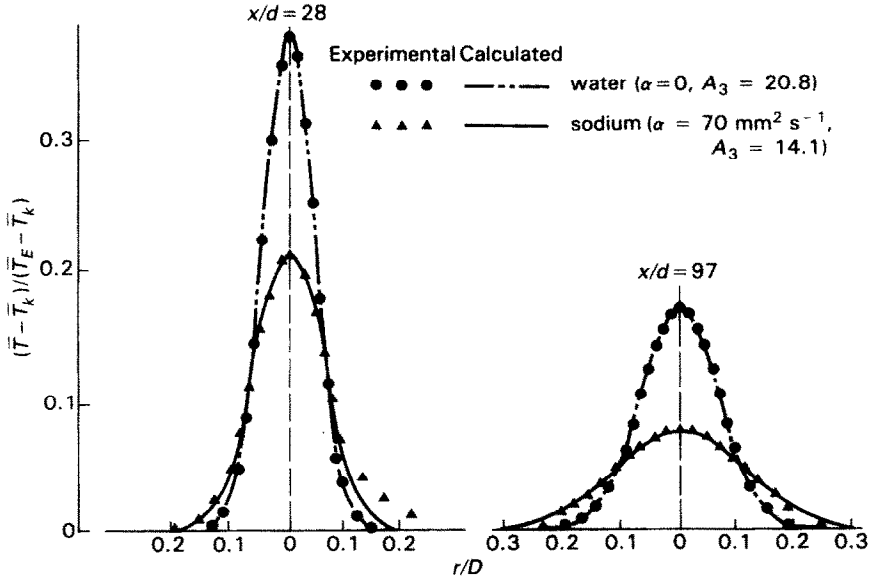

FIG. 5. Radial mean temperature profiles—$Re_M = 34\,140$.

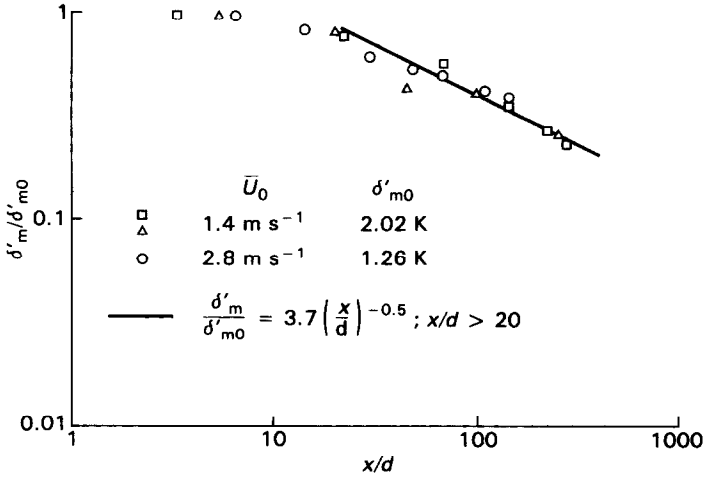

FIG. 6. Decay of temperature fluctuations in water.

negative which is in general agreement with the results reported for water in ref. [13]. A similar trend was observed for the lateral velocity fluctuation in air. Flatness factors for both u and v are close to three for the measurement domain up to $x/d = 150$. Triple products $\overline{u^2v}$ and $\overline{uv^2}$ were measured in air. For $x/d < 15$ both are negative with a value of -0.35 for $\overline{u^2v}/u'^2v'$ and $\overline{uv^2}/u'v'^2$ at $x/d = 3.3$. At large x/d, both triple products vanished.

Similarly, a non-zero cross-correlation coefficient existed between u and v for some radial positions about the centreline of a bore for $x/d < 30$ but vanished further downstream. The sign and magnitude of the cross-correlation near the jet block exit are directly related to the flow issuing from a bore in the jet block since such a flow closely approaches developed pipe flow due to the large length-to-diameter ratio of the bores.

5. DISCUSSION OF RESULTS

Although model parameters in equations (7) and (12) have been derived qualitatively with the assumption of flow homogeneity and power law decay of velocity turbulence components, excellent predictions of mean and fluctuating temperatures were obtained by use of experimental temperature data obtained at only one plane. Of particular interest is modelling of the temperature fluctuation dissipation term of equation (8). Commonly used models introduce the time

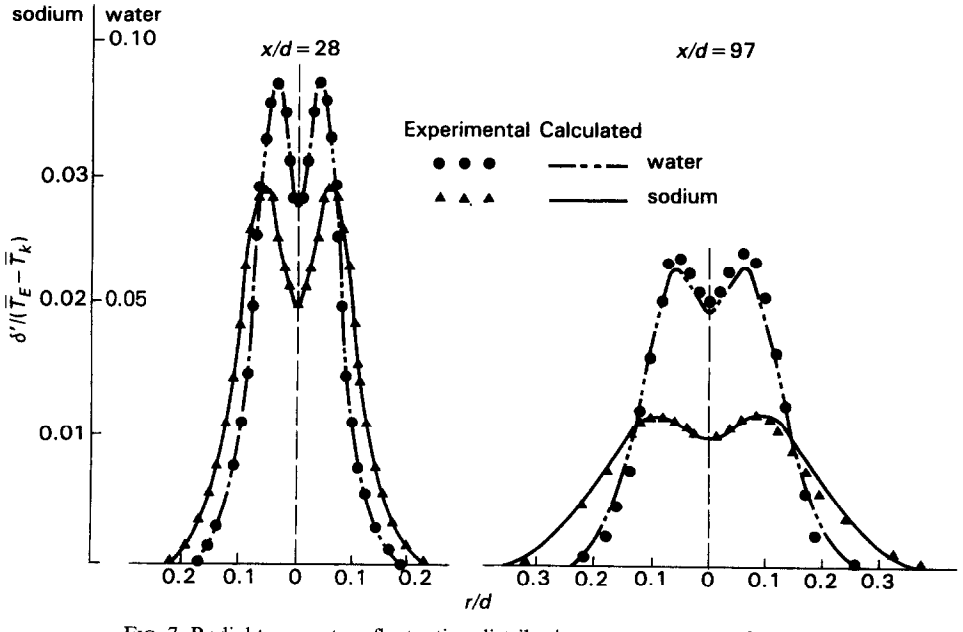

FIG. 7. Radial temperature fluctuation distributions—parameters as for Fig. 8.

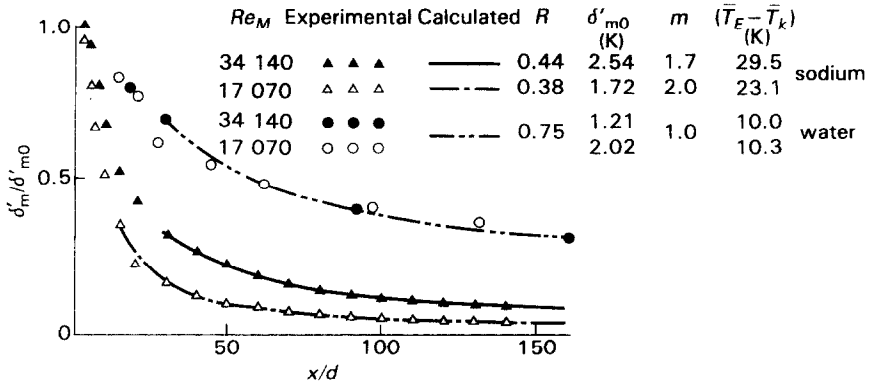

FIG. 8. Axial decay of maximum intensity of temperature fluctuations.

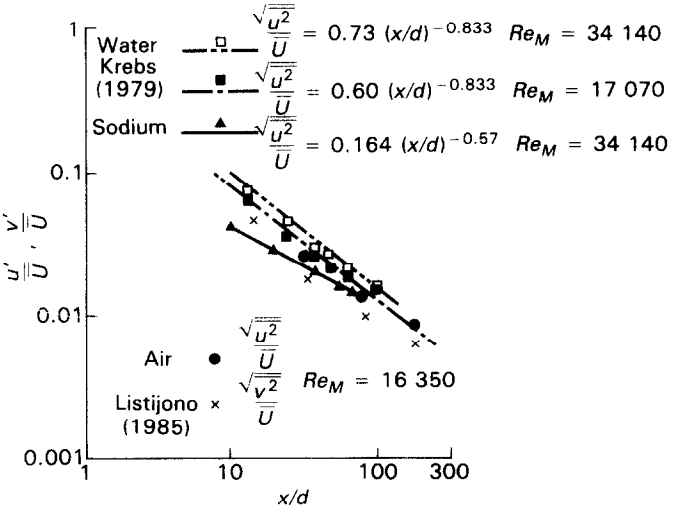

FIG. 9. Axial decay of turbulence intensities.

scale ratio of equation (10) which is assumed to have a universal value. Since modelling parameters used in the present work give excellent fits to measured temperature data, it is seen that with $n_1 = 1.67$ for all cases, the best value of R is 0.75 for both cases with water but 0.38 and 0.44 for low and high Reynolds numbers, respectively, for liquid sodium.

These values of R are in broad agreement with the recommended value of 0.5 for shear flows and 0.833 for grid flows [8], but the deviations are significant, as $\bar{\delta}^2$ computed from equation (11) or equation (12) is sensitive to the dissipation term containing R. Furthermore, the distinctly different values for sodium and water, indicate a Prandtl number dependence which has been highlighted by the widely different values of thermal diffusivity of sodium and water. More advanced modelling [14], introduces transport equations for dissipation of velocity and scalar fluctuations. Although these models were developed for the case of $Pr \approx 1$ and homogeneous flow, a Prandtl number effect is present since each transport equation contains purely turbulence related terms plus one molecular term. The latter leads to the Prandtl number effect on R.

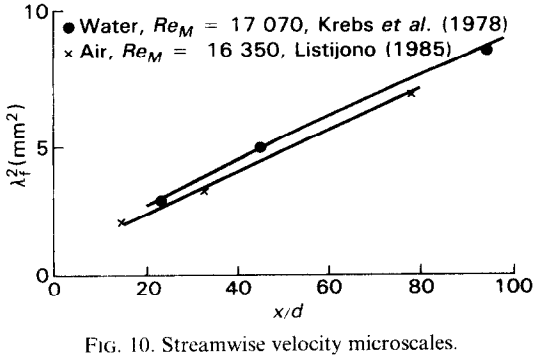

FIG. 10. Streamwise velocity microscales.

The sensitivity of temperature fluctuation predictions to changes in R can be studied by observing the corresponding changes in δ'. For water at $x/d = 96$, a doubling of R increases δ' at the centreline by 64% whereas halving R leads to a reduction of 63%. Similar changes are observed for various radii

thus yielding a similar distribution to those of Fig. 7 but at different levels. The corresponding result for sodium is an increase of only 34% and a decrease of 38%.

6. CONCLUSIONS

Simplified transport equations for mean and fluctuating temperature have been modelled for flow behind a multi-bore jet block used to simulate flow in the exit plenum of liquid metal cooled nuclear reactor fuel rod subassemblies. Model parameters were developed with the assumption of power law decay of turbulence energy with downstream distance from the jet block. Values of parameters were obtained with the aid of experimental data at only one plane in the case of the fluctuating temperature field. Solution of the transport equations then gave excellent agreement with experimental data at other points in the flow.

Values of parameters determined from experimental data can be used as a check against those obtained by others. In particular, since the temperature field is nonhomogeneous, a valuable check of modelling of temperature fluctuation dissipation through a dissipation time scale ratio, is available. For water a time scale ratio of 0.75, whereas for liquid sodium a value of 0.38–0.44, depending on Reynolds number, was found appropriate. These values can be compared with those of 0.833 for grid turbulence, and 0.5 for shear flows [8].

An electromagnetic probe used for streamwise velocity fluctuation measurements in liquid sodium was found to suffer slightly from lack of adequate spatial resolution but generally confirmed measurements in water and air for this geometry and hence the model assumptions.

Measurements performed with air, confirmed microscale measurements in water but also showed the whole flow field to be nonisotropic as judged by a 20% difference between streamwise and lateral turbulence intensities. Near the jet block a non-zero correlation coefficient between u and v was found as well as non-zero values of third-order velocity moments.

REFERENCES

1. G. Comte-Bellot and S. Corrsin, The use of a contraction to improve the isotropy of grid-generated turbulence, *J. Fluid Mech.* **25**(4), 657–682 (1966).
2. Z. Warhaft and J. L. Lumley, The decay of temperature fluctuations and heat flux in grid generated turbulence, Symposium on Turbulence, Technical University, Berlin, 1–5 August (1977). *Lect. Notes in Phys.* No. 76 (Edited by H. Fiedler), pp. 113–123. Springer, Berlin (1978).
3. R. S. Brodkey, *Turbulence in Mixing Operations*, Chaps 2 and 3. Academic Press, New York (1975).
4. M. Gad-el-Hak and J. B. Morton, Experiments on the diffusion of smoke in isotropic turbulent flow, *AIAA J.* **17**, 558–562 (1979).
5. L. Krebs, K. Bremhorst and U. Müller, Measurement and prediction of the mean and fluctuating temperature field downstream of a multi-bore jet block in which one jet is heated, *Int. J. Heat Mass Transfer* **24**, 1305–1312 (1981).
6. S. Corrsin, Heat transfer in isotropic turbulence, *J. Appl. Phys.* **23**, 113–118 (1952).
7. L. Krebs, Ausbreitung von Temperaturstörungen in begrenzter Strömung hinter einem Düsenblock, Dr.-Ing. Dissertation, University of Karlsruhe (TH) (1979).
8. P. Bradshaw, T. Cebeci and J. H. Whitelaw, *Engineering Calculation Methods for Turbulent Flow*. Academic Press, New York (1981).
9. D. B. Spalding, Concentration fluctuations in a round turbulent jet, *Chem. Engng Sci.* **26**, 95 (1971).
10. St. Müller, L. Krebs and G. Thun, Permanent magnet flow meter probes, sensors for instrumentation in LMFBRs, Int. Topical Meeting on Liquid Metal Fast Breeder Reactor Safety and Related Design, Lyon, 19–23 July (1982).
11. K. Bremhorst, Effect of fluid temperature on hot-wire anemometers and an improved method of temperature compensation and linearisation without use of small signal sensitivities, *J. Phys. E: Sci. Instrum.* **18**(1), 44–49 (1985).
12. J. B. H. Listijono, Velocity fields behind a multi-bore jet block, M.Eng.Sci. thesis, University of Queensland, St. Lucia, Australia (1985).
13. L. Krebs, K. Bremhorst and U. Müller, Measurements of thermal diffusion downstream of a multi-bore jet block, Symposium on Turbulence, Technical University, Berlin, 1–5 August (1977). *Lect. Notes in Phys.* No. 76 (Edited by H. Fiedler), pp. 101–112. Springer, Berlin (1978).
14. G. R. Newman, B. E. Launder and J. L. Lumley, Modelling the behaviour of homogeneous scalar turbulence, *J. Fluid Mech.* **111**, 217–232 (1981).

APPLICATION D'UN MODELE DE DIFFUSION DE GRADIENT ET DE RAPPORT D'ECHELLE DE TEMPS DE DISSIPATION A LA PREDICTION DES CHAMPS DE TEMPERATURE MOYENNE ET FLUCTUANTS DANS LE SODIUM LIQUIDE EN AVAL D'UN BLOC A PLUSIEURS TROUS

Résumé—Un modèle antérieur basé sur la diffusivité pour la prédiction des températures moyennes et fluctuantes dans un écoulement d'eau en aval d'un bloc percé de plusieurs trous d'où sortent des jets dont l'un d'eux est chaud, est appliqué à un écoulement de sodium dans un appareil de forme semblable. Quelques mesures, difficiles dans le sodium ou l'eau pour cette géométrie, sont faites avec l'air de façon à vérifier les hypothèses faites dans le modèle. Le modèle mathématique antérieur est modifié pour placer des hypothèses sur le nombre de Reynolds de turbulence et le nombre de Péclet de turbulence dans le relation entre les microéchelles de vitesse et de température. On teste le modèle de Spalding qui relie les taux de dissipation des fluctuations de vitesse et de température. On identifie un effet sensible du faible nombre de Prandtl du sodium liquide. Des mesures faites sur l'air, derrière le bloc à plusieurs jets, vérifient la nature non isotrope de l'écoulement à large échelle. Les résultats montrent clairement que les mesures faites dans l'eau peuvent être transférées au sodium liquide à condition d'inclure la diffusion moléculaire dans l'équation de la température moyenne, en tenant compte de l'effet du faible nombre de Prandtl sur le rapport d'échelle de temps de dissipation et du coefficient de diffusion des fluctuations de moyenne quadratique de température, qui est supposé égal à la diffusivité turbulente de la chaleur.

BERECHNUNG VON MITTLEREN UND FLUKTUIERENDEN TEMPERATURVERTEILUNGEN IN FLÜSSIGEM NATRIUM STROMABWÄRTS EINES VIELFACH DURCHBOHRTEN STRAHLBLOCKS MITTELS EINES GRADIENTENVERFAHRENS

Zusammenfassung—Ein früher entwickeltes, auf der Temperaturleitfähigkeit basierendes Modell zur Berechnung mittlerer und fluktuierender Temperaturen in Wasser stromabwärts eines vielfach durchbohrten Strahlblocks, in dem ein Strahl beheizt wird, wird angewandt auf einen Natriumstrom in einer Apparatur ähnlicher Geometrie. Für einige Messungen, die in fließendem Natrium oder Wasser nicht so einfach durchgeführt werden können, wird Luft verwendet; damit werden die dem Modell zugrundelegten Annahmen überprüft. Das früher entwickelte mathematische Modell wird verändert, um Annahmen über die turbulente Reynolds-Zahl und die turbulente Peclet-Zahl in der Beziehung zwischen der Geschwindigkeits- und Temperatur-Mikroskala überflüssig zu machen. Das Modell von Spalding, welches Fluktuationsgeschwindigkeit und Temperaturdissipationsrate in Beziehung setzt, wird überprüft. Dabei zeigt die geringe Prandtl-Zahl des flüssigen Natriums einen gewichtigen Einfluß auf diese Beziehung. Messungen hinter einem vielfach durchbohrten, mit Luft als Arbeitsmedium betriebenen Strahlblock haben bestätigt, daß die makroskopische Strömung nicht isotrop ist. Die Ergebnisse zeigen eindeutig, daß in Wasser durchgeführte Messungen auf flüssiges Natrium übertragen werden können, vorausgesetzt, daß die molekulare Diffusion in die Gleichung für die mittlere Temperatur einbezogen wird, daß für den Einfluß der Prandtl-Zahl auf das Dissipationszeitskalenverhältnis ein Spielraum gewährt wird und schließlich der Koeffizient der Gradientendiffusion des mittleren Quadrats der Temperaturfluktuationen gleich der turbulenten Temperaturleitfähigkeit angenommen wird.

ПРИМЕНЕНИЕ МОДЕЛИ ОТНОШЕНИЯ ВРЕМЕННЫХ МАСШТАБОВ ГРАДИЕТНОЙ ДИФФУЗИИ И ДИССИПАЦИИ ДЛЯ РАСЧЕТА ПОЛЕЙ СРЕДНЕЙ И КОЛЕБАТЕЛЬНОЙ ТЕМПЕРАТУР ПРИ НИСХОДЯЩЕМ ТЕЧЕНИИ НАТРИЯ В МНОГОКАНАЛЬНОМ БЛОКЕ

Аннотация—Разработнная ранее и основанная на температуропроводности модель для расчета средних и колебательных температур нисходящего потока воды в многоканальном блоке, одна из струй в котором нагревается, используется для описания течения натрия в аналогичном устройстве. Некоторые измерения, которые трудно осуществить при течении натрия или воды, выполнены с использованием воздуха для подтверждения используемых в модели предположений. Ранее предложенная математическая модель модифицирована таким образом, чтобы можно было исключить предположения о турбулентных числах Рейнольдса и Пекле в зависимости между микромасштабами скорости и температуры. Проверена модель Сполдинга, устанавливающая зависимость между колебательной скоростью и интенсивностью диссипации тепла. Обнаружено существенное влияние низкого значения числа Прандтля жидкого натрия на эту зависимость. Измерения, проведенные в струе воздуха после выхода из блока, подтвердили неизотропный характер крупномасштабного потока. Результаты наглядно показывают, что проведенные в воде измерения можно применить и к жидкому натрию при условии, что в уравнении для средней температуры учитывается молекулярная диффузия, а также что учитывается влияние числа Прандтля на характерные временные масштабы диссипации, и принимается, что коэффициент градиентной диффузии среднеквадратичных колебаний температуры равен коэффициенту турбулентной диффузии.